THE JOURNAL OF BIOLOGICAL CHEMISTRY VOL. 286, NO. 17, pp. 14744–14752, April 29, 2011

Monocarboxylate Transporter-1 Is Required for Cell Death in Mouse Chondrocytic ATDC5 Cells Exposed to Interleukin-1β via Late Phase Activation of Nuclear Factor κB and Expression of Phagocyte-type NADPH Oxidase*[S]

Received for publication, January 13, 2011 Published, JBC Papers in Press, March 3, 2011, DOI 10.1074/jbc.M111.221259

Kentaro Yoshimura[‡], Yoichi Miyamoto[‡1], Rika Yasuhara[§], Toshifumi Maruyama[‡¶], Tomohito Akiyama[‡¶], Atsushi Yamada[‡], Masamichi Takami[‡], Tetsuo Suzawa[‡], Shoko Tsunawaki[‖], Tetsuhiko Tachikawa[§], Kazuyoshi Baba[¶], and Ryutaro Kamijo[‡]

From the Departments of [‡]Biochemistry, [§]Oral Pathology and Diagnosis, and [¶]Prosthodontics, Showa University School of Dentistry, Tokyo 142-8555, Japan and the [‖]Department of Infectious Diseases, National Research Institute for Child Health and Development, Tokyo 157-8535, Japan

Interleukin-1β (IL-1β) induces cell death in chondrocytes in a nitric oxide (NO)- and reactive oxygen species (ROS)-dependent manner. In this study, increased production of lactate was observed in IL-1β-treated mouse chondrocytic ATDC5 cells prior to the onset of their death. IL-1β-induced cell death in ATDC5 cells was suppressed by introducing an siRNA for monocarboxylate transporter-1 (MCT-1), a lactate transporter distributed in plasma and mitochondrial inner membranes. *Mct-1* knockdown also prevented IL-1β-induced expression of phagocyte-type NADPH oxidase (NOX-2), an enzyme specialized for production of ROS, whereas it did not have an effect on inducible NO synthase. Suppression of IL-1β-induced cell death by *Nox-2* siRNA indicated that NOX-2 is involved in cell death. Phosphorylation and degradation of inhibitor of κBα (IκBα) from 5 to 20 min after the addition of IL-1β was not affected by *Mct-1* siRNA. In addition, IκBα was slightly decreased after 12 h of incubation with IL-1β, and the decrease was prominent after 36 h, whereas activation of p65/RelA was observed from 12 to 48 h after exposure to IL-1β. These changes were not seen in *Mct-1*-silenced cells. Forced expression of IκBα super repressor as well as treatment with the IκB kinase inhibitor BAY 11-7082 suppressed NOX-2 expression. Furthermore, *Mct-1* siRNA lowered the level of ROS generated after 15-h exposure to IL-1β, whereas a ROS scavenger, *N*-acetylcysteine, suppressed both late phase degradation of IκBα and *Nox-2* expression. These results suggest that MCT-1 contributes to NOX-2 expression via late phase activation of NF-κB in a ROS-dependent manner in ATDC5 cells exposed to IL-1β.

Degeneration of articular cartilage is commonly observed in the pathogenesis of joint diseases, such as rheumatoid arthritis and osteoarthritis. One of the most prominent changes in cartilage affected by these diseases is loss of extracellular matrix due to its elevated degradation and lowered synthesis (1), whereas reduced cellularity in cartilage is another feature (2, 3). It is known that proinflammatory cytokines, such as tumor necrosis factor-α (TNF-α) and interleukin-1β (IL-1β), produced by synovial cells and chondrocytes, play pivotal roles in the progression of these degenerative changes, in part by stimulating the production of reactive nitrogen and oxygen species (ROS)[2] in an autocrine/paracrine mechanism. Such reactive intermediates are regarded as causal or contributing factors for these diseases (1, 4–6).

In our previous study, we demonstrated that IL-1β induces cell death in rat primary chondrocytes and mouse chondrocytic ATDC5 cells via mitochondrial dysfunction in a nitric oxide (NO)- and ROS-dependent manner (7). Furthermore, expression of the inducible type of NO synthase (NOS-2), a characteristic of chondrocytes (8), was induced by IL-1β within a few h in these cells. Formation of peroxynitrite, a reaction product of NO and superoxide ($O_2^{\cdot-}$), was reported to be one of the executioners of cell death (5–7), which indicates the importance of increased production of $O_2^{\cdot-}$ in these cells.

Several biological systems are known to produce ROS, including $O_2^{\cdot-}$, namely, the mitochondrial electron transfer system, the arachidonate cascade, xanthine oxidase, uncoupled NO synthases, and NADPH oxidases (NOXs). Among those, we previously observed the progression of cell death as increments of NOX-2 expression in IL-1β-treated chondrocytes (7). NOXs are enzymes specialized for generation of $O_2^{\cdot-}$ and H_2O_2, and seven members of the NOX family have been identified thus far, including NOX-1, -2, -3, -4, and -5 and Duox-1 and -2 (9). Among them, NOX-2 is the best characterized and reported to be mainly distributed in phagocytes, such as macrophages, neutrophils, and dendritic cells. The function of

* This work was supported by Grant-in-aid for Scientific Research 21592372 from the Japan Society for the Promotion of Science and by the High-Tech Research Center Project for Private Universities from the Ministry of Education, Culture, Sports, Science, and Technology, Japan, 2005–2009.

[S] The on-line version of this article (available at http://www.jbc.org) contains supplemental Figs. S1 and S2.

[1] To whom correspondence should be addressed: 1-5-8 Hatanodai, Shinagawa-ku, Tokyo 142-8555, Japan. Fax: 81-3-3784-8163; E-mail: yoichim@dent.showa-u.ac.jp.

[2] The abbreviations used are: ROS, reactive oxygen species; NOX, NADPH oxidase; MCT, monocarboxylate transporter; DCFH-DA, 2′,7′-dichlorodihydrofluorescin diacetate; αCHC, α-cyano-4-hydroxycinnamate; L-NAME, N^{ω}-nitro-L-arginine methyl ester; MTT, 3-(4,5-dimethylthiazol-2-yl)-2,5-diphenyl-2H-tetrazolium bromide; MTS, 3-(4,5-dimethylthiazol-2-yl)-5-(3-carboxymethoxyphenyl)-2-(4-sulfophenyl)-2H-tetrazolium, inner salt; NAC, *N*-acetyl-L-cysteine; IKK, IκB kinase.

NOX-2 in these cells is regulated by its activation via assembly of the components of the NOX enzyme system, which are NOX-2, $p22^{phox}$, $p40^{phox}$, $p47^{phox}$, $p67^{phox}$, and Rac (9). In addition to the antiseptic functions of NOX-2 in these immune cells, attention is increasingly being focused on the diverse biological actions of NOX enzymes in various types of cells (9).

Although the expression of NOX enzymes in chondrocytes has not been fully clarified, a NOX-2 homologue and NOX complex have been observed in porcine articular chondrocytes and a human chondrocyte line (10, 11), in addition to our observation described above (7). Recently, it was reported that TNF-α, interferon-γ, and lipopolysaccharide induced the expression of *Nox-2* via activation of nuclear factor κB (NF-κB) in murine and human phagocytes (12, 13). However, to the best of our knowledge, there are no reports regarding the regulatory mechanism of *Nox-2* expression in chondrocytes.

In the present study, we observed activation of NF-κB in ATDC5 cells after prolonged exposure to IL-1β. Both late phase activation of NF-κB and induction of *Nox-2* expression in IL-1β-treated ATDC5 cells were found to be dependent on monocarboxylate transporter (MCT)-1, a transmembrane transporter for lactate and pyruvate (14). MCTs are distributed in plasma membrane and catalyze transmembrane transport of monocarboxylates. Among the 14 genes identified as MCT isoforms, seven of them have been characterized so far. Because MCT-1, -2, -3, and -4 transport monocarboxylates, such as lactate and pyruvate, with H^+, depending on their intra- and extracellular concentrations, they are considered to constitute a part of energy metabolism as well as that of the pH regulatory system. MCT-6 transports diuretics, depending on pH and membrane potential. MCT-10 transports aromatic amino acids, depending on their concentration gradients. It is known that MCT-1, -2, and -4 are distributed not only in plasma membrane but also in mitochondrial inner membrane. Among these MCT isoforms, MCT-1 is ubiquitously expressed and regarded to play an important role in oxidative energy production (14). Herein, we describe the role of MCT-1 in NF-κB activation and *Nox-2* induction in ATDC5 cells.

EXPERIMENTAL PROCEDURES

Reagents—Recombinant mouse IL-1β was obtained from R&D Systems (Minneapolis, MN). α-Cyano-4-hydroxycinnamate (αCHC), N^{ω}-nitro-L-arginine methyl ester (L-NAME), and 3-(4,5-dimethylthiazol-2-yl)-2,5-diphenyl-2H-tetrazolium bromide (MTT) were purchased from Sigma-Aldrich. A CellTiter 96® Aqueous One Solution cell proliferation assay, which contains a water-soluble derivative of MTT, 3-(4,5-dimethylthiazol-2-yl)-5-(3-carboxymethoxyphenyl)-2-(4-sulfophenyl)-2H-tetrazolium, inner salt (MTS) (15), came from Promega (Madison, WI). *N*-Acetyl-L-cysteine (NAC) and 2′,7′-dichlorodihydrofluorescin diacetate (DCFH-DA) were from WAKO Pure Chemical Industries (Osaka, Japan) and Dojindo Laboratories (Kumamoto, Japan), respectively. BAY11-7082, PD98059, and MG-132, inhibitors of κB (IκB) kinase (IKK), MEK, and proteasomes, respectively, were purchased from Merck. Antibodies against IκBα and phospho-IκBα were obtained from Cell Signaling Technology (Beverly, MA). The antibody against NF-κB p65/RelA was purchased from Santa Cruz Biotechnology, Inc. (Santa Cruz, CA), and that for β-actin was obtained from Sigma-Aldrich.

Cell Culture—ATDC5 cells (16) were supplied by the Riken BioResource Center (Tsukuba, Japan) and maintained in DMEM/F-12 containing 2.5% fetal calf serum (FCS) (MP Biomedicals LLC, Solon, OH), 100 units/ml penicillin G, 100 μg/ml streptomycin, and 0.25 μg/ml amphotericin B. In some experiments, ATDC5 cells were precultured for 2 weeks in the presence of ITS (10 μg/ml insulin, 5.5 μg/ml transferrin, 6.7 ng/ml sodium selenite) (Invitrogen) and used as differentiated ATDC5 cells.

Introduction of siRNA—Stealth™ siRNAs for mouse *Mct-1*, *Mct-6*, *Mct-13*, and *Nox-2* and their control non-silencing siRNAs were purchased from Invitrogen. The siRNAs (30 pmol) were introduced into 40–50% confluent cells in 6-well plates using Lipofectamine™ RNAiMAX (Invitrogen) by reverse transfection.

Forced Expression of IκB Super Repressor—Addgene plasmid 15291, harboring a gene for the IκBα super repressor, pBABE-puro-IKBα-mut (17), and Addgene plasmid 1764 (pBABE-puro) (18) were supplied by Addgene Inc. (Cambridge, MA). ATDC5 cells were infected with retroviruses generated by BOSC 23 cells that had been transfected with these plasmids, as described previously (19).

Cell Viability—Cells were plated in 96-well plates at various densities and then treated with IL-1β (10 ng/ml) in complete medium containing 2.5% FCS. Cell viability was assessed using an MTT assay after incubation for 4 h with 0.5 mg/ml MTT. Formed MTT-formazan was solubilized in isopropyl alcohol containing 40 mM HCl and determined by reading absorbance at 562 nm using a microplate reader (SH-1000 Lab, Corona Electric Co., Ltd., Ibaraki, Japan). In some experiments, cells were incubated for 1 h with solution from a CellTiter 96® Aqueous One Solution cell proliferation assay kit, and then MTS-formazan was determined by reading absorbance at 490 nm. Cell viability was also evaluated by counting the number of adherent cells. Cells were fixed in 10% formalin-PBS, rinsed in PBS, and stained with 0.05% toluidine blue at pH 7.0 for 30 min. After rinsing in tap water, the number of cells was counted using cell counting software preinstalled in a BZ-9000 microscope (Keyence Co., Osaka, Japan).

Determination of Lactate Concentration—Cells were cultured for 24 or 48 h in complete medium in the presence (10 ng/ml) or absence of IL-1β. Lactate concentrations in the culture supernatants were determined using an L-lactic acid UV test (R-Biopharm AG, Darmstadt, Germany), according to the manufacturer's instructions.

Evaluation of ROS Generation—Cells were incubated with 10 μM DCFH-DA in the dark for 2 h at 37 °C (20). They were harvested by collagenase digestion, washed three times with PBS containing 0.2% bovine serum albumin (BSA), and resuspended in Hanks' balanced solution containing 0.2% BSA. ROS-dependent fluorescence of 2′,7′-dichlorodihydrofluorescein from the cell suspension was determined using a FACSCaliber Flow cytometer (BD Biosciences).

RT-PCR—Total RNA was extracted from the cells using TRIzol® solution (Invitrogen), according to the manufacturer's instructions. Reverse transcription reactions were performed

using Superscript III (Invitrogen) and a random hexamer. The primers for PCR were designed using Primer3 software (21) based on the sequences of mouse glyceraldehyde-3-phosphate dehydrogenase (GAPDH), *Nox-2*, and the *Mct* isoforms, which were synthesized and supplied by Invitrogen. The sequences of the primers used and the amplicon sizes of the genes are as follows: GAPDH, 5′-ACC ACA GTC CAT GCC ATC AC-3′ and 5′-TCC ACC ACC CTG TTG CTG TA-3′ (452 bp); *Nox-2*, 5′-GAG GGT TTC CAG CCA GCG AAC TTT GGT-3′ and 5′-TGA AGG GGG CCT GTA TGT GG-3′ (349 bp); *Mct-1*, 5′-GCT GGA GGT CCT ATC AGC AG-3′ and 5′-CGG ACA GCT TTT CTC CTT TG-3′ (502 bp); *Mct-2*, 5′-TTA CCG TAT CTG GGC CTT TG-3′ and 5′-CCA AAG CAG TTT CGA AGG AG-3′ (462 bp); *Mct-3*, 5′-ACG GCT GGT TTC ATA ACA GG-3′ and 5′-CCA TTT TTC TCA GGC TCT GC-3′ (530 bp); *Mct-4*, 5′-CAT CGA AGT GCA AGG AGA CA-3′ and 5′-TTT GAT CAG CAA TCC ATC CA-3′ (414 bp); *Mct-6*, 5′-CTT TCG CTA CCG AGT TCT GG-3′ and 5′-CCA CGA CGT GAA AAT GTG TC-3′ (461 bp); *Mct-7*, 5′-CGT CCA CGA ATC CAG TAC CT-3′ and 5′-TGT GCG TTT GAA GCT TTG AC-3′ (491 bp); *Mct-8*, 5′-GTG CTT TCG TGG TGT ACG TG-3′ and 5′-TCT CAG CCT CCA CAT CCT CT-3′ (773 bp); *Mct-9*, 5′-ACG GGA GAC TTC CCT TCC TA-3′ and 5′-CAG GAC ACA GAA GCC ACT GA-3′ (676 bp); *Mct-10*, 5′-CTG CTC CCT TTG CTG TTA GG-3′ and 5′-CTT CAC ACC GGG CAA ATA GT-3′ (426 bp); *Mct-12*, 5′-TGT CGT TCA GCT CCT CAT TG-3′ and 5′-GGA AGG TTT GAA GCA TTG GA-3′ (545 bp); *Mct-13*, 5′-GGC CCT CTT GCT AGT GTC TG-3′ and 5′-AGT TCA GGA AGC ACG GAG AA-3′ (486 bp); and *Mct-14*, 5′-CAC CAA CCG CAT GTT TGT AG-3′ and 5′-CAA AGA TCC ATC CTG CGA AT-3′ (366 bp). The PCR products were separated on a 1.0% agarose gel and stained with ethidium bromide.

Real-time RT-PCR—Quantitative real-time RT-PCR was performed using TaqMan™ Gene Expression Assays (Applied Biosystems, Carlsbad, CA). The amplification signals from the target genes were normalized against that of GAPDH.

Western Blot Analysis—Cells were lysed in 10 mM Tris-HCl (pH 7.8) containing 1% Nonidet P-40, 0.15 M NaCl, and a protease inhibitor mixture containing EDTA (Roche Applied Science). The cell lysates (5 μg of protein) were subjected to SDS-PAGE (10% polyacrylamide gel) under a reducing condition. Following electrophoresis, proteins were transferred onto PVDF membranes and incubated overnight at 4 °C with the primary antibodies against phospho-IκBα and IκBα, followed by incubation with horseradish peroxidase-conjugated anti-rabbit IgG (GE Healthcare). Immunoreactive bands were visualized by an enhanced chemiluminescence reaction with an ECL plus Western blot detection system (GE Healthcare).

Activation of p65/RelA—Nuclear extracts were prepared using a nuclear extraction kit (Active Motif Inc., Carlsbad, CA). Active p65/RelA in the nuclear extracts was quantitatively analyzed using a TransAM™ NF-κB p65 transcription factor assay kit (Active Motif Inc.), which is an ELISA-based quantification system for p65/RelA bound to κB oligonucleotide. In addition, subcellular localization of p65/RelA was assessed using an immunocytochemical method. Briefly, cells were fixed for 20 min with 2% paraformaldehyde in PBS at room temperature

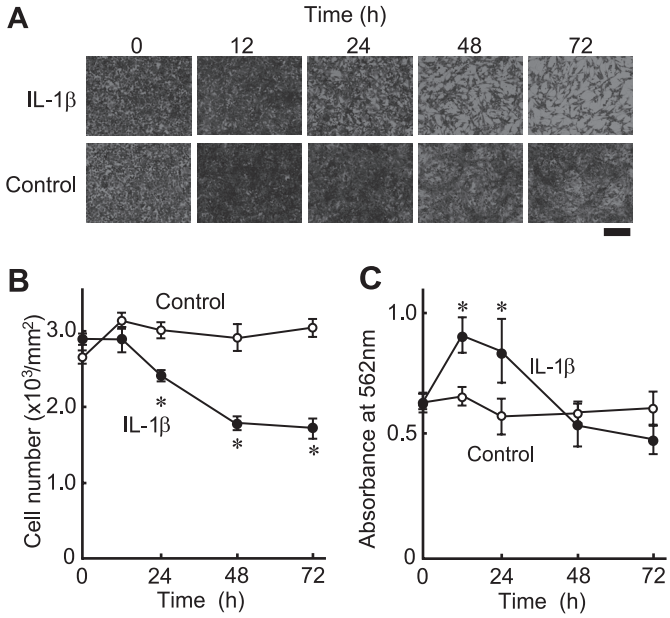

FIGURE 1. **IL-1β-induced cell death in ATDC5 cells.** ATDC5 cells were plated in 96-well plates at a density of 1×10^5 cells/well and then cultured in complete medium in the presence or absence of IL-1β (10 ng/ml). *A* and *B*, cells were stained with toluidine blue at the indicated time points. *A*, representative photographs are shown. *Scale bar*, 200 μm. *B*, the number of cells was counted at each time point. ○, cells cultured in the absence of IL-1β; ●, cells cultured in the presence of IL-1β. *C*, cell viability was evaluated using an MTT assay. ○, cells cultured in the absence of IL-1β. ●, cells cultured in the presence of IL-1β. *B* and *C*, results are shown as the mean ± S.D. (*error bars*) of four independent experiments. *, $p < 0.05$.

and permeated with 0.1% Triton X-100 in PBS for 5 min. Next, the cells were incubated overnight at 4 °C with 1 μg/ml anti-p65/RelA rabbit antibody in PBS containing 10% goat serum, followed by incubation with Alexafluor®-488-conjugated secondary antibody (Invitrogen) diluted in PBS (1:100) for 45 min at room temperature. Fluorescence was observed using a BZ-9000 microscope.

Statistical Analysis—Data are expressed as the mean ± S.D. Student's *t* test was used for statistical analysis, with $p < 0.05$ considered to be significant.

RESULTS

IL-1β-induced Cell Death in ATDC5 Cells—ATDC5 cells were plated at a density of 1×10^5 cells/well in 96-well plates and then cultured in the presence or absence of IL-1β (10 ng/ml) for up to 72 h. Cell viability was assessed based on the number of adherent cells stained with toluidine blue. Time-dependent cell death was observed after exposure to IL-1β (Fig. 1, *A* and *B*). The percentage of living cells after 24 h was 80% of that of the control cells, which decreased gradually over 72 h to 57% of the control (Fig. 1*B*). Cell viability was also evaluated by an MTT assay, one of the commonly used methods to assess cell proliferation and cell death. MTT assay results are mainly based on the reduction of MTT tetrazolium salt by the mitochondrial electron transfer system (21). The MTT-reducing activities of cells treated for 12 and 24 h with IL-1β were 1.4- and 1.5-fold greater, respectively, than those of the control cells, which showed that IL-1β increased the MTT-reducing activity of the cells by 55% at 12 h and 75% at 24 h (Fig. 1*C*). Considering that MTT is mainly reduced by the mitochondrial electron trans-

port system (21), it is conceivable that IL-1β increased the activity of the mitochondrial electron transfer system within the initial 12 h. However, cell viability evaluated by MTT assays continued to decline with IL-1β treatment after 24 h (Fig. 1*C*). Together, these results indicate that IL-1β not only suppresses the proliferation of ATDC5 cells but also induces cell death after prolonged incubation for longer than 24 h.

To examine the effects of the cell density and differentiation stage on IL-1β-induced cell death, ATDC5 cells maintained in undifferentiated conditions, and those differentiated by 2-week cultures in the presence of ITS were treated with IL-1β. The expressions of mRNAs for typical differentiation markers (*i.e.* aggrecan, type II collagen, and type X collagen) as well as those for IL-1β and its receptor were assessed by RT-PCR after culturing at various densities for 48 h in the presence or absence of IL-1β (10 ng/ml) (supplemental Fig. S1). Both differentiated ATDC5 cells and those maintained in undifferentiated stage until used for experiments expressed type II collagen mRNA after 48 h of culture in a confluent state, whereas IL-1β suppressed the expressions of type II and type X collagens. In all of the experimental conditions, IL-1β mRNA was hardly detected in ATDC5 cells. On the other hand, the expression of mRNA for IL-1 receptor in the cells in the undifferentiated state was higher than that in the differentiated state, especially at higher cell density. In addition, IL-1β slightly induced the expression of its receptor in undifferentiated cells (supplemental Fig. S1).

ATDC5 cells maintained in undifferentiated state and those differentiated by ITS treatment were seeded into 96-well plates at a density of 6×10^4 and 6×10^3 cells/well (*i.e.* nearly confluent and one-tenth confluent, respectively). Next, they were treated with IL-1β (10 ng/ml), and viability was examined by counting the numbers of cells as well as measuring the reduction of MTS, a water-soluble derivative of MTT (15) (supplemental Fig. S2). In a nearly confluent state (6×10^4 cells/well), both undifferentiated and differentiated ATDC5 cells began to die after incubation for more than 24 h with IL-1β. (supplemental Fig. S2, *A* and *B*, *top panels*). Although formation of MTS formazan in the undifferentiated and differentiated cells increased after 24 h of incubation with IL-1β, it was greater in the undifferentiated ATDC5 cells (supplemental Fig. S2, *A* and *B*, *bottom panels*). As for cells in a one-tenth confluent state (6×10^3 cells/well), the increase in the number of undifferentiated cells was significantly suppressed by IL-1β, whereas such suppression was not significant in the differentiated cells (supplemental Fig. S2, *C* and *D*, *top panels*). Furthermore, MTS reduction was not affected by IL-1β treatment in either undifferentiated or differentiated cells (supplemental Fig. S2, *C* and *D*, *bottom panels*).

These results are summarized as follows. IL-1β augmented MTT/MTS reduction, *Nox-2* expression, and cell death in ATDC5 cells both in low and high differentiated stages, when they were cultured at high densities. However, the efficacy of IL-1β to induce MTT/MTS reduction and cell death was dependent on cell density and differentiation, with both more prominent in lower differentiated cells in a higher density state. Therefore, we investigated the mechanism of IL-1β-induced cell death in confluent ATDC5 cells that had been maintained in the undifferentiated state before use.

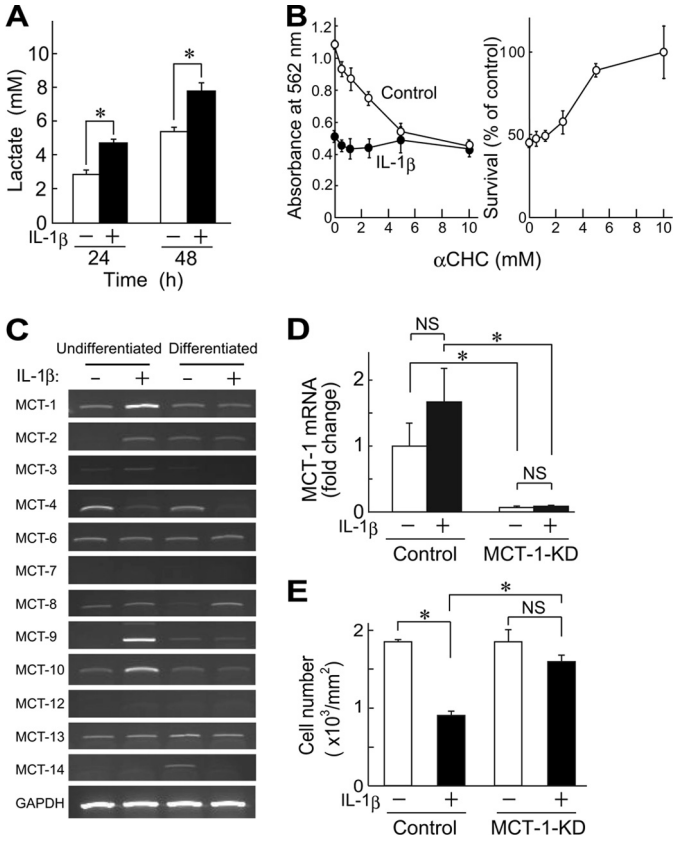

FIGURE 2. **Involvement of MCT-1 in IL-1β-induced cell death.** *A*, ATDC5 cells were cultured for 24 or 48 h in the presence or absence of IL-1β (10 ng/ml), after which lactate concentrations in the culture supernatants were determined. *Black* and *white columns* show results obtained in cultures with and without IL-1β, respectively. *B*, ATDC5 cells were incubated with IL-1β (10 ng/ml) for 48 h in the presence of various concentrations of αCHC, an inhibitor of MCT. Cell viability was assessed using an MTT method. *Left*, absorbance of MTT-formazan formed in control (○) and IL-1β-treated cells (●). *Right*, results shown in the *left panel* are presented as the percentage of control cells cultured without IL-1β in the presence of αCHC. *C*, the expressions of mRNAs for *Mct* isoforms were assessed by RT-PCR. Total RNA was isolated from undifferentiated and differentiated ATDC5 cells after culturing for 48 h in the presence or absence of IL-1β (10 ng/ml). *D*, the expression of *Mct-1* was suppressed by introducing its siRNA (*MCT-1-KD*). ATDC5 cells introduced with *Mct-1* siRNA were incubated for 48 h with or without IL-1β (10 ng/ml). Signals from the target genes were normalized against that of GAPDH. The results are expressed as values relative to that obtained from the control cells (*far left column*). *E*, *Mct-1*-silenced cells (*MCT-1-KD*) and control cells (6×10^4 cells/well) were incubated for 60 h with IL-1β (10 ng/ml). Cell viability was assessed by counting the number of adherent cells after toluidine blue staining. *A*, *B*, *D*, and *E*, results are shown as the mean ± S.D. (*error bars*) of four independent experiments. *, $p < 0.05$. *NS*, not significant.

Involvement of MCT-1 in Cell Death Induced by IL-1β—Interestingly, IL-1β increased the concentration of lactate in culture supernatants of ATDC5 cells over 24 h (Fig. 2*A*). It is known that short-chain carboxylates, such as lactate and pyruvate, are transported across the plasma membrane and mitochondrial inner membrane via proton-linked MCTs (23). Therefore, IL-1β is considered to augment lactate production in ATDC5 cells. Recently, several reports have described the biological significance of lactate and MCTs in mitochondrial production of ROS and inflammatory responses (24, 25). Thus, we examined the effect of an MCT inhibitor, αCHC, on IL-1β-induced cell death in ATDC5 cells. αCHC suppressed MTT-formazan formation in a concentration-dependent manner (Fig. 2*B*, *left*), possibly due to lowered energy metabolism (21).

When the values obtained in the presence of IL-1β were normalized by those obtained in the absence of the cytokine, αCHC appeared to have a protective effect on ATDC5 cells against IL-1β-induced cell death, which implies possible involvement of MCT subtypes involved in IL-1β-elicited death of ATDC5 cells.

Among the 14 known *Mct* gene subtypes (26), expressions of mRNAs for *Mct-1*, *-2*, *-4*, *-6*, *-8*, *-9*, *-10*, *-13*, and *-14* were detected in undifferentiated and differentiated ATDC5 cells in both the presence and absence of IL-1β (Fig. 2*C*). Furthermore, IL-1β augmented the expression of *Mct-1*, *-9*, and *-10* and suppressed that of *Mct-4* in undifferentiated ATDC5 cells. MCT-1, -2, and -4 are reported to be inhibited by αCHC (27); thus, MCT-1 is considered to be the most abundant subtype among those susceptible to αCHC, especially in undifferentiated ATDC5 cells treated with IL-1β. Thus, we also investigated the role of MCT-1 in IL-1β-induced gene expression and cell death in ATDC5 cells by introducing siRNA for *Mct-1*, which nearly completely suppressed the expression of *Mct-1* mRNA both in the presence and absence of IL-1β (Fig. 2*D*). In addition, *Mct-1* siRNA significantly suppressed cell death in ATDC5 cells after exposure to IL-1β for 48 h (Fig. 2*E*).

Involvement of NOX-2 in IL-1β-induced Cell Death—Our previous findings indicated that peroxynitrite, a reaction product of NO and O_2^-, plays a pivotal role in IL-1β-induced cell death in rat primary chondrocytes as well as ATDC5 cells (7). In those experimental conditions, augmented expressions of NOS-2 and NOX-2 were observed, and their inhibitors suppressed cell death (7). In the present study, we examined the effects of *Mct-1* knockdown on IL-1β-induced expression of mRNAs for *Nos-2* and *Nox-2*. Introduction of *Mct-1* siRNA did not have an effect on IL-1β-induced expression of *Nos-2* (Fig. 3*A*), whereas it significantly suppressed that of *Nox-2* (Fig. 3*B*). On the other hand, introduction of siRNAs for other MCT subtypes, such as *Mct-6* and *Mct-13*, did not have a distinct effect on NOX-2 expression or cell death after IL-1β treatment (data not shown).

To elucidate the link between suppression of cell death and reduction of *Nox-2* expression by *Mct-1* knockdown, we also examined the effect of *Nox-2* silencing on IL-1β-dependent cell death in ATDC5 cells. As shown in Fig. 3*C*, cell death was significantly suppressed in cells introduced with the *Nox-2* siRNA, thus confirming the involvement of NOX-2 in IL-1β-induced cell death in ATDC5 cells.

As shown in supplemental Fig. S1, the expression of *Nox-2* mRNA was prominent in ATDC5 cells in a lower differentiation stage at higher density as compared with differentiated cells or cells at a lower density. Because undifferentiated ATDC5 cells at higher density tended to die following IL-1β treatment (supplemental Fig. S2), the speculation that NOX-2 plays an important role in IL-1β-induced cell death was reinforced. Lower expression of IL-1 receptor in the differentiated cells might contribute, in part, to the cause of weaker *Nox-2* induction in those cells.

Regulation of Late Phase IκBα Degradation and Expression of Nox-2 by MCT-1—It was recently reported that NF-κB is involved in transcription of *Nox-2* in both murine and human phagocytes (12, 13). In particular, p65/RelA-dependent transcription of the *Nox-2* gene was confirmed in murine monocytes (12). We examined the phosphorylation and degradation of IκBα in ATDC5 cells in a nearly confluent state. As shown in Fig. 4*A*, IL-1β induced the phosphorylation and degradation of IκBα 5–20 min after IL-1β stimulation in both the control and *Mct-1* siRNA-introduced ATDC5 cells. These results indicate that MCT-1 is not involved in this immediate response.

On the other hand, it should be noted that IκBα was slightly decreased from 12 to 24 h and then disappeared after 48 h of incubation with IL-1β in ATDC5 cells harboring the control siRNA (Fig. 4*A*, *left*), whereas the level of IκBα was maintained during this period in the cells introduced with *Mct-1* siRNA (Fig. 4*A*, *right*). A more detailed time course investigation of the degradation of IκBα and expression of *Nox-2* mRNA from 24 to 48 h after the addition of IL-1β was performed (Fig. 4*B*). In the control ATDC5 cells, a marked decrease in IκBα protein was observed from 36 h after the addition of IL-1β to the culture. Furthermore, *Nox-2* mRNA expression was seen at a low level from 24 to 32 h and then became intense after 36 h (Fig. 4*B*, *left*). On the other hand, both the decrease in IκBα protein and increase in *Nox-2* mRNA were minimal during the same period in cells introduced with *Mct-1* siRNA (Fig. 4*B*, *right*). In contrast, the expression of IκBα mRNA in ATDC5 cells was not affected by either treatment with IL-1β or introduction of *Mct-1* siRNA (data not shown), indicating that the decrease in level of IκBα protein in cells treated with IL-1β was probably due to its degradation.

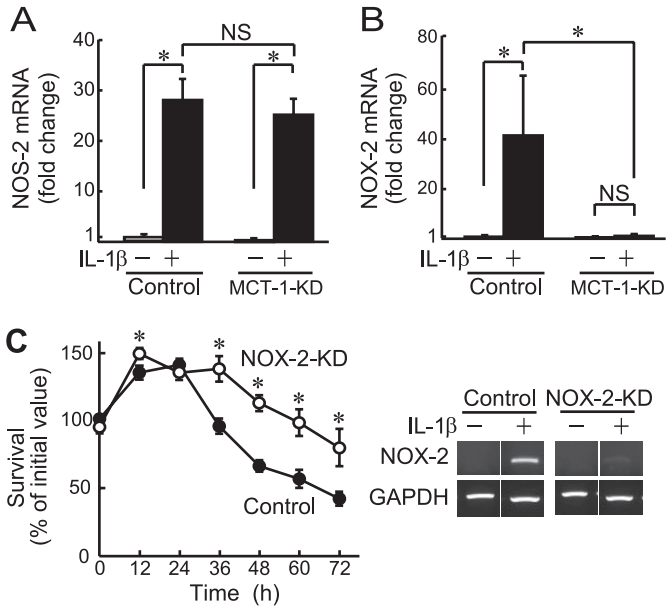

FIGURE 3. **Involvement of NOX-2 in IL-1β-induced cell death.** *A* and *B*, the expressions of mRNAs for *Nos-2* (*A*) and *Nox-2* (*B*) were quantitatively analyzed by real-time RT-PCR in *Mct-1*-silenced (*MCT-1-KD*) and control ATDC5 cells with or without treatment with IL-1β (10 ng/ml) for 48 h. Amplification signals from the target genes were normalized against that from GAPDH. The results are shown as values relative to that obtained from the control cells (*far left column*). *C*, *Nox-2*-silenced (*NOX-2-KD*) and control ATDC5 cells were plated at a density of 6.0×10^4 cells/well and cultured for the indicated periods in the presence of IL-1β (10 ng/ml). Cell viability was evaluated using an MTT assay. ○, *Nox-2*-silenced cells. ●, control cells. *Right*, the expression of *Nox-2* mRNA in control siRNA- and *Nox-2* siRNA-introduced ATDC5 cells (*NOX-2-KD*) was assessed by RT-PCR after incubation for 48 h with IL-1β (10 ng/ml). *A–C*, results are expressed as the mean ± S.D. (*error bars*) of four independent experiments. *, $p < 0.05$. *NS*, not significant.

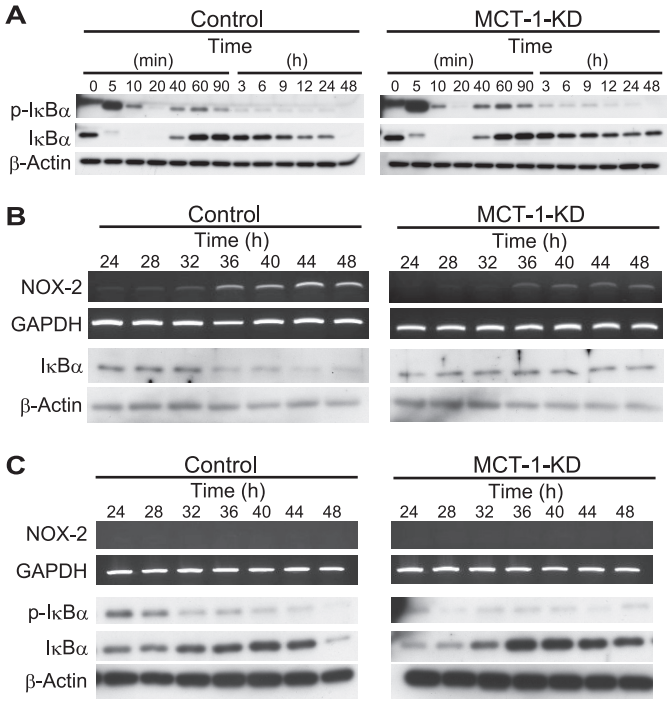

FIGURE 4. **Involvement of MCT-1 in IL-1β-induced IκBα degradation and *Nox-2* expression.** *A*, phosphorylation and degradation of IκBα after treatment with IL-1β (10 ng/ml) in control (*left*) and *Mct-1*-silenced (*MCT-1-KD*) ATDC5 cells (*right*) at various time points were examined by Western blotting. IκBα disappeared after 48 h in the control cells, whereas it remained in the *Mct-1*-silenced cells. *B*, a more precise study of the time courses of *Nox-2* expression and IκBα degradation was performed in the period from 24 to 48 h after the addition of IL-1β in the control (*left*) and *Mct-1*-silenced (*MCT-1-KD*) ATDC5 cells (*right*). *C*, inhibition of IκBα degradation and *Nox-2* expression by a proteasome inhibitor, MG-132. Control (*left*) and *Mct-1*-silenced (*MCT-1-KD*) ATDC5 cells (*right*) were treated for the indicated periods with IL-1β (10 ng/ml). MG-132 (5 μM) was added to the culture 4 h before each isolation of total RNA and protein fractions from cells at the indicated time points. The expression of *Nox-2* mRNA was examined by RT-PCR, whereas those of phospho-IκBα (*p-IκBα*) and IκBα were assessed by Western blotting.

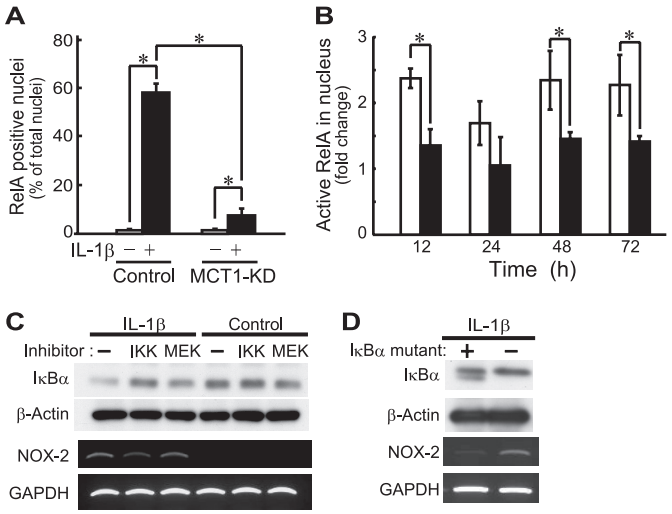

FIGURE 5. **Involvement of MCT-1 in IL-1β-induced activation of p65/RelA.** *A*, the subcellular distribution of p65/RelA was examined by specific immunostaining at 48 h after treatment with IL-1β. The percentage of cells with p65/RelA localized in the nucleus is expressed as the mean ± S.D. (*error bars*) of four independent experiments. *, $p < 0.05$. *B*, control siRNA-introduced (*unfilled columns*) and *Mct-1* siRNA-introduced (*filled columns*) cells were incubated with IL-1β (10 ng/ml) for the indicated time periods. Active p65/RelA in nuclear extracts was determined by ELISA-based quantification of p65/RelA bound to κB oligonucleotide. See "Results" for details. *C*, ATDC5 cells were cultured for 48 h in the presence or absence of IL-1β (10 ng/ml). At 24 h after the addition of IL-1β, an IKK inhibitor, BAY 11-7082 (2.5 μM) (*IKK*), an MEK inhibitor, PD98059 (50 μM) (*MEK*), or the vehicle alone (−) was added to the culture. *Top panels*, protein levels of IκBα and β-actin were assessed by Western blotting. *Bottom panels*, the expressions of mRNAs for *Nox-2* and GAPDH were assessed by RT-PCR. *D*, cells were infected with retroviruses harboring an IκBα mutant, the NF-κB super repressor, or a control virus for 24 h. After selection of the infected cells by 24 h of incubation with puromycin, cells were further incubated for 48 h with IL-1β (10 ng/ml). Expressions of IκBα and β-actin (*top*) and those of *Nox-2* and GAPDH (*bottom*) were assessed by Western blotting and RT-PCR, respectively.

To ascertain the involvement of proteasomes in down-regulation of IκBα protein expression in IL-1β-treated cells, we examined the effects of a proteosome inhibitor, MG-132, on the levels of phospho-IκBα and IκBα in IL-1β-treated ATDC5 cells with or without introduction of *Mct-1* siRNA (Fig. 4*C*). MG-132 suppressed the decrease in IκBα level until 44 h after IL-1β treatment in the control siRNA-introduced cells. However, the suppression of disappearance of IκBα by MG-132 was partial at 48 h, indicating a possible involvement of mechanisms other than the degradation by proteasomes in the decrease in IκBα at that time point. We detected phospho-IκBα during the period 24–44 h after IL-1β treatment by Western blotting in both control and *Mct-1*-silenced cells in the presence of MG-132 (Fig. 4*C*), whereas phospho-IκBα was hardly detected in its absence (Fig. 4*A*). These results indicate that degradation of phospho-IκBα by proteasomes was responsible, at least in part, for the decrease in IκBα level after prolonged incubation with IL-1β (Fig. 4, *A* and *B*).

Although nuclear translocation of p65/RelA was detected in control ATDC5 cells incubated with IL-1β for 48 h, that in the *Mct-1*-silenced cells was clearly suppressed (Fig. 5*A*). More specifically, after 48 h of incubation with IL-1β (10 ng/ml), only 8% of *Mct-1*-silenced cells had p65/RelA-positive nuclei, whereas 58% of the control cells showed nuclear translocation of p65/RelA with the same stimulation. Next, we performed a time course study of p65/RelA activation using an ELISA-based quantification kit for active p65/RelA (TransAM^{TM} NF-κB p65, Active Motif). As shown in Fig. 5*B*, nuclear active p65/RelA was increased within 12 h after the addition of IL-1β in the control siRNA-introduced ATDC5 cells and was retained until 48 h. On the other hand, the increase in the amount of active p65/RelA in *Mct-1*-silenced cells was significantly lower than that in the control cells.

To confirm the involvement of the NF-κB pathway in the induced expression of *Nox-2* in IL-1β-treated ATDC5 cells, we examined the effects of the IκBα super repressor pBABE-puro-IKBα-mut as well as an IKK inhibitor, BAY11-7082, on *Nox-2* expression. The expression of *Nox-2* mRNA and disappearance of IκBα in ATDC5 cells after 48 h of treatment with IL-1β were suppressed by BAY11-7082, whereas these were not affected by an MEK inhibitor, PD98059 (Fig. 5*C*). In addition, forced expression of the IκBα super repressor inhibited IL-1β-induced expression of NOX-2 mRNA in ATDC5 cells (Fig. 5*D*). These results indicate that the IκBα-p65/RelA axis is involved in IL-1β-induced expression of *Nox-2* in ATDC5 cells.

Involvement of ROS in IL-1β-induced Expression of Nox-2 mRNA—Numerous studies have indicated that ROS are involved in the activation of NF-κB. In addition, it was recently reported that increased NF-κB-dependent gene expression in

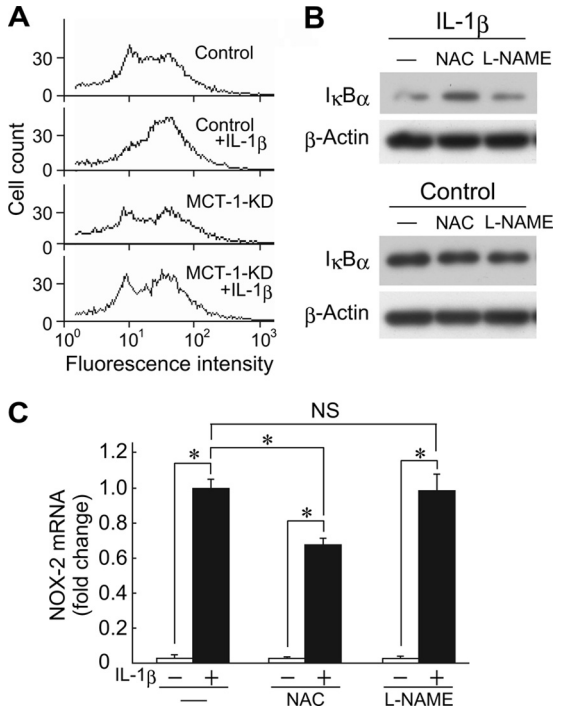

FIGURE 6. **Involvement of ROS in late phase activation of NF-κB after IL-1β treatment.** *A*, control and *Mct-1*-silenced (*MCT-1-KD*) ATDC5 cells were cultured for 15 h in the presence or absence of IL-1β (10 ng/ml). The amount of ROS was measured using flow cytometry. *B*, ATDC5 cells were cultured for 48 h in the presence or absence of IL-1β (10 ng/ml). At 24 h after the addition of IL-1β, NAC (5 mM) or L-NAME (5 mM) was added to the culture. The protein levels of IκBα and β-actin were assessed by Western blotting. *C*, ATDC5 cells were cultured for 48 h in the presence or absence of IL-1β (10 ng/ml). At 24 h after the addition of IL-1β, NAC (5 mM) or L-NAME (5 mM) was added to the culture. The expressions of mRNAs for *Nox-2* and GAPDH after 48 h of incubation with IL-1β were assessed by real-time RT-PCR. Amplification signals from the *Nox-2* gene were normalized to that from the GAPDH gene. The results are shown as values relative to those obtained from cells exposed to IL-1β in the absence of NAC or L-NAME. Results are expressed as the mean ± S.D. (*error bars*) of four independent experiments. *, $p < 0.05$. *NS*, difference is not significant.

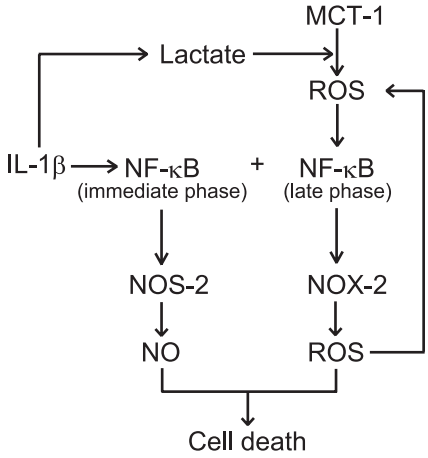

FIGURE 7. **Schematic diagram of MCT-1-dependent NF-κB activation and NOX-2 expression.** IL-1β immediately activates the NF-κB pathway, which may be involved in the expression of NOS-2. On the other hand, IL-1β augments the production of lactate, which causes generation of ROS in an MCT-1-dependent manner. ROS in turn induce late phase activation of NF-κB, which is required for expression of NOX-2. ROS participate in late phase activation of NF-κB. In our previous report (7), we found that IL-1β-induced cell death required augmented production of both NO and ROS. In the present study, the participation of NOX-2 in cell death was indicated.

cells exposed to lactate was inhibited by αCHC (25). Therefore, we examined the production of ROS in ATDC5 cells after treatment with IL-1β. Although IL-1β elevated ROS production in ATDC5 cells with intact *Mct-1* expression, it did not affect ROS production in *Mct-1*-silenced cells (Fig. 6*A*). To examine the involvement of ROS and NO in degradation of IκBα and induction of *Nox-2* transcription, ATDC5 cells were treated with IL-1β for 48 h in the presence or absence of NAC, a scavenger of ROS, or L-NAME, an NOS inhibitor for 24–48 h. NAC suppressed the late phase degradation of IκBα induced after 48 h of treatment with IL-1β (Fig. 6*B*), and NAC suppressed IL-1β-induced expression of *Nox-2* mRNA (Fig. 6*C*), whereas L-NAME did not have effects on either. These results indicate that ROS play an important role in IκBα degradation and *Nox-2* expression in IL-1β-treated ATDC5 cells. On the other hand, NO, despite its earlier production, is scarcely involved in *Nox-2* induction.

DISCUSSION

In the present study, we found that IL-1β induced biphasic activation of the canonical NF-κB pathway in chondrocytic ATDC5 cells. Late phase NF-κB activation following prolonged exposure to IL-1β was involved in the expression of *Nox-2*, which contributed to cell death induced by the cytokine. In addition, we found that MCT-1 was required for onset of late phase activation of NF-κB and, hence, expression of *Nox-2*. It is likely that ROS produced in an *Mct-1*-dependent fashion play an important role in the activation of NF-κB. Our speculation regarding this process is summarized in Fig. 7.

It is known that ROS and reactive nitrogen species are involved in degradation of articular cartilage, including chondrocyte death, in degenerative joint diseases, such as rheumatoid arthritis, and osteoarthritis (4–6). We previously reported that peroxynitrite, a highly reactive compound formed by the reaction of NO and O_2^-, induced necrotic cell death in ATDC5 cells and primary rat chondrocytes via mitochondrial dysfunction after exposure to IL-1β. In those experimental settings, NOS-2 expression was induced within 6 h, whereas the onset of NOX-2 expression was observed after a longer period of treatment with IL-1β (7). In the present study, introduction of a *Nox-2* siRNA significantly suppressed IL-1β-dependent cell death in ATDC5 cells (Fig. 3*C*). These results indicate that ROS, including O_2^- and/or H_2O_2, produced by NOX-2 are involved, at least in part, in cell death, although the involvement of ROS produced by enzymes or biological systems other than NOX-2 cannot be ruled out. The possibility also exists that NOX-2 plays a role in the vicious cycle of ROS generation in IL-1β-treated ATDC5 cells, as described in earlier reports that used different experimental systems (12, 28, 29).

It is well known that the expression of *Nos-2* is induced in chondrocytes by a single inflammatory cytokine, such as interferon-γ, tumor necrosis factor-α, or IL-1β (8). On the other hand, the expression of *Nox-2* by chondrocytes has not been fully investigated. The expression of *Nox-2* by neutrophils as well as *Nos-2* by various types of cells has been reported to be induced under the regulation by NF-κB (12, 13, 30). In the present study, biphasic activation of NF-κB was observed in ATDC5 cells following exposure to IL-1β (Fig. 4*A*). More specifically,

phosphorylation and degradation of IκBα, or the so-called canonical pathway, was observed immediately after stimulation with IL-1β, followed by later activation of NF-κB, which was shown by the disappearance of IκBα and activation of p65/RelA (Figs. 4 and 5). Non-canonical pathways have been shown to be involved in prolonged activation of NF-κB (31, 32). Although participation of non-canonical pathways remains to be studied, the canonical pathway for NF-κB was activated in ATDC5 cells after prolonged exposure to IL-1β.

It is noteworthy that *Mct-1* knockdown suppressed both late phase degradation of IκBα and activation of p65/RelA (Figs. 4 and 5), whereas it did not have an effect on immediate phosphorylation or degradation of IκBα (Fig. 4). *Mct-1* knockdown also inhibited the expression of *Nox-2*, whereas it did not affect that of *Nos-2* (Fig. 3, *A* and *B*). These results indicate that late phase activation of NF-κB in IL-1β-treated ATDC5 cells is important for expression of *Nox-2*, whereas the immediate activation of NF-κB may play a role in NOS-2 expression. In addition, MCT-1 is required for late phase, but not immediate, activation of NF-κB.

MCT-1 transports lactate and pyruvate across plasma membranes inward or outward, depending on the intracellular and extracellular concentrations of these monocarboxylates and H^+ (14). An increase in lactate production in cytosol facilitates excretion of lactate and H^+ through MCT-1 to prevent intracellular acidification (26). In the present study, lactate concentration in the culture supernatants was significantly increased after 24 h of incubation with IL-1β (Fig. 2*A*), indicating an increased intracellular concentration of lactate at that time point. Although the mechanisms related to how IL-1β elevates lactate production in ATDC5 cells remain to be elucidated, it is possible that IL-1β accelerates glucose metabolism to produce lactate, as has been observed in human chondrocytes (33). The augmented production of lactate seen at 24 h after IL-1β treatment indicates that it is involved in IκBα degradation, p65/RelA activation, NOX-2 expression, and cell death.

It is also known that MCT-1 is distributed in mitochondrial inner membranes as a component of a complex with lactate dehydrogenase, cytochrome *c* oxidase, and CD147 (23). Previous studies have suggested that this complex facilitates the conversion of lactate to pyruvate and hence the supply of pyruvate to mitochondrial matrix as a substrate for ROS generation as well as for energy production (23, 24). In our study, we observed augmented reduction of MTT in cells treated with IL-1β for 12 or 24 h (Fig. 1*C*). A previous report noted that 77% of total MTT reduction occurred in mitochondria, 80% of which was carried out on complex IV of the electron transfer system, when succinate was used as a substrate (22). Therefore, it is plausible that lactate, the concentration of which was increased in the cytosol of IL-1β-treated ATDC5 cells, is used to facilitate MTT reduction in mitochondria after transportation through the complex containing MCT-1.

A previous study found that lactate augments NF-κB-mediated gene expression via MCTs through the production of ROS (25). ROS is generated in mitochondria as a by-product of the electron transport system (34), and it is well documented that NF-κB is a redox-sensitive transcription factor (35–37). In the present study, inhibition of IL-1β-induced *Nox-2* expression and IκBα degradation by NAC indicated the involvement of ROS in these phenomena (Fig. 6). Generation of ROS in ATDC5 cells was slightly augmented after 15 h of incubation with IL-1β, which was not observed in *Mct-1*-silenced cells (Fig. 6*A*). These results indicate that an increase in cytosolic lactate augments ROS generation in mitochondria in an *Mct-1*-dependent manner. NO reportedly inhibits IKKβ through its nitrosylation and hence inhibits the NF-κB pathway (38). However, in our study, L-NAME did not have an effect on *Nox-2* expression (Fig. 6, *B* and *C*), indicating that the involvement of NO in regulation of *Nox-2* expression is minimal.

In contrast to the marked disappearance of IκBα and *Nox-2* expression after incubation with IL-1β for 36 h (Fig. 4), activation of p65/RelA was observed in the control siRNA-introduced cells from 12 h, which was significantly suppressed in *Mct-1*-silenced cells (Fig. 5*B*). It has been reported that ROS activate NF-κB via both canonical (36) and non-canonical (32) pathways. In addition, it was recently reported that IKKβ functions as an adaptor protein that facilitates nuclear translocation of the p65/RelA-p50-IκBα complex in UV-irradiated cells (39). There is a possibility that ROS produced in IL-1β-treated ATDC5 cells induces IKKβ-dependent nuclear translocation of p65/RelA in a complex with IκBα at 12 h after IL-1β treatment, which leads to activation of p65/RelA thereafter. Inhibition of *Nox-2* transcription by an IKK inhibitor as well as the IκBα super repressor suggests that p65/RelA activation dependent on degradation of IκBα plays an important role in this process (Fig. 5). Compared with the marked accumulation of p65/RelA in the nucleus (Fig. 5*A*), the increment in the amount of active p65/RelA in the nucleus was only 2-fold after IL-1β treatment (Fig. 5*B*). For that reason, it seems likely that an appreciable amount of nuclear p65/RelA existed as a complex with IκBα. Further studies are required for clarification of this issue.

The present results show that MCT-1 is required for expression of *Nox-2*, which plays an important role in cell death of ATDC5 cells exposed to IL-1β. MCT-1 is involved in the production of ROS, which in turn activate NF-κB and induce *Nox-2* transcription. It is conceivable that ROS derived from NOX-2 are able to augment generation of ROS from mitochondria (29). Furthermore, NOX-2-dependent activation of NF-κB has been reported (28). Our present findings along with those of previous reports indicate that MCT-1 plays an important role in formation of the vicious cycle of oxidative stress in chondrocytes in inflammatory conditions. Therefore, MCT-1 is a potential target for regulation of degenerative joint diseases.

REFERENCES

1. Goldring, M. B., and Marcu, K. B. (2009) *Arthritis Res. Ther.* **11,** 224
2. Kim, H. A., and Blanco, F. J. (2007) *Curr. Drug Targets* **8,** 333–345
3. Del Carlo, M., Jr., and Loeser, R. F. (2008) *Curr. Rheumatol. Rep.* **10,** 37–42
4. Daheshia, M., and Yao, J. Q. (2008) *J. Rheumatol.* **35,** 2306–2312
5. Del Carlo, M., Jr., and Loeser, R. F. (2002) *Arthritis Rheum.* **46,** 394–403
6. Whiteman, M., Armstrong, J. S., Cheung, N. S., Siau, J. L., Rose, P., Schantz, J. T., Jones, D. P., and Halliwell, B. (2004) *FASEB J.* **18,** 1395–1397
7. Yasuhara, R., Miyamoto, Y., Akaike, T., Akuta, T., Nakamura, M., Takami, M., Morimura, N., Yasu, K., and Kamijo, R. (2005) *Biochem. J.* **389,** 315–323
8. Maier, R., Bilbe, G., Rediske, J., and Lotz, M. (1994) *Biochim. Biophys. Acta* **1208,** 145–150
9. Bedard, K., and Krause, K. H. (2007) *Physiol. Rev.* **87,** 245–313

10. Moulton, P. J., Hiran, T. S., Goldring, M. B., and Hancock, J. T. (1997) *Br. J. Rheumatol.* **36,** 522–529
11. Henrotin, Y. E., Bruckner, P., and Pujol, J. P. (2003) *Osteoarthr. Cartil.* **11,** 747–755
12. Anrather, J., Racchumi, G., and Iadecola, C. (2006) *J. Biol. Chem.* **281,** 5657–5667
13. Gauss, K. A., Nelson-Overton, L. K., Siemsen, D. W., Gao, Y., DeLeo, F. R., and Quinn, M. T. (2007) *J. Leukoc. Biol.* **82,** 729–741
14. Halestrap, A. P., and Price, N. T. (1999) *Biochem. J.* **343,** 281–299
15. Cory, A. H., Owen, T. C., Barltrop, J. A., and Cory, J. G. (1991) *Cancer Commun.* **3,** 207–212
16. Shukunami, C., Ishizeki, K., Atsumi, T., Ohta, Y., Suzuki, F., and Hiraki, Y. (1997) *J. Bone Miner. Res.* **12,** 1174–1188
17. Boehm, J. S., Zhao, J. J., Yao, J., Kim, S. Y., Firestein, R., Dunn, I. F., Sjostrom, S. K., Garraway, L. A., Weremowicz, S., Richardson, A. L., Greulich, H., Stewart, C. J., Mulvey, L. A., Shen, R. R., Ambrogio, L., Hirozane-Kishikawa, T., Hill, D. E., Vidal, M., Meyerson, M., Grenier, J. K., Hinkle, G., Root, D. E., Roberts, T. M., Lander, E. S., Polyak, K., and Hahn, W. C. (2007) *Cell* **129,** 1065–1079
18. Morgenstern, J. P., and Land, H. (1990) *Nucleic Acids Res.* **18,** 3587–3596
19. Krebs, D. L., Yang, Y., Dang, M., Haussmann, J., and Gold, M. R. (1999) *Methods Cell Sci.* **21,** 57–68
20. De Clerck, L. S., Bridts, C. H., Mertens, A. M., Moens, M. M., and Stevens, W. J. (1994) *J. Immunol. Methods* **172,** 115–124
21. Rozen, S., and Skaletsky, H. J. (2000) *Methods Mol. Biol.* **132,** 365–386
22. Berridge, M. V., and Tan, A. S. (1993) *Arch. Biochem. Biophys.* **303,** 474–482
23. Hashimoto, T., Hussien, R., and Brooks, G. A. (2006) *Am. J. Physiol. Endocrinol. Metab.* **290,** E1237–E1244
24. Hashimoto, T., Hussien, R., Oommen, S., Gohil, K., and Brooks, G. A. (2007) *FASEB J.* **21,** 2602–2612
25. Samuvel, D. J., Sundararaj, K. P., Nareika, A., Lopes-Virella, M. F., and Huang, Y. (2009) *J. Immunol.* **182,** 2476–2484
26. Helestrap, A. P., and Meredith, D. (2004) *Pflügers Arch.* **447,** 619–628
27. Morris, M. E., and Felmlee, M. A. (2008) *AAPS J.* **10,** 311–321
28. Clark, R. A., and Valente, A. J. (2004) *Mech. Ageing Dev.* **125,** 799–810
29. Frein, D., Schildknecht, S., Bachschmid, M., and Ullrich, V. (2005) *Biochem. Pharmacol.* **70,** 811–823
30. Ganster, R. W., and Geller, D. A. (2000) in *Nitric Oxide Biology and Pathology* (Ignarro, L. J., ed) pp. 129–156, Academic Press, Inc., San Diego, CA
31. Saitoh, T., Nakayama, M., Nakano, H., Yagita, H., Yamamoto, N., and Yamaoka, S. (2003) *J. Biol. Chem.* **278,** 36005–36012
32. Cristofanon, S., Morceau, F., Scovassi, A. I., Dicato, M., Ghibelli, L., and Diederich, M. (2009) *FASEB J.* **23,** 45–57
33. Shikhman, A. R., Brinson, D. C., and Lotz, M. K. (2004) *Am. J. Physiol. Endocrinol. Metab.* **286,** E980–E985
34. Kowaltowski, A. J., de Souza-Pinto, N. C., Castilho, R. F., and Vercesi, A. E. (2009) *Free Radic. Biol. Med.* **47,** 333–343
35. Kamata, H., Manabe, T., Oka, S., Kamata, K., and Hirata, H. (2002) *FEBS Lett.* **519,** 231–237
36. Gloire, G., Legrand-Poels, S., and Piette, J. (2006) *Biochem. Pharmacol.* **72,** 1493–1505
37. Enesa, K., Ito, K., Luong, L. A., Thorbjornsen, I., Phua, C., To, Y., Dean, J., Haskard, D. O., Boyle, J., Adcock, I., and Evans, P. C. (2008) *J. Biol. Chem.* **283,** 18582–18590
38. Perkins, N. D. (2006) *Oncogene* **25,** 6717–6730
39. Tsuchiya, Y., Asano, T., Nakayama, K., Kato, T., Jr., Karin, M., and Kamata, H. (2010) *Mol. Cell* **39,** 570–582